Photon-Photon Entanglement with a Single Trapped Atom

B. Weber, H. P. Specht, T. Müller, J. Bochmann, M. Mücke, D. L. Moehring,* and G. Rempe
Max-Planck-Institut für Quantenoptik, Hans-Kopfermann-Strasse 1, 85748 Garching, Germany
(Received 11 September 2008; published 20 January 2009)

An experiment is performed where a single rubidium atom trapped within a high-finesse optical cavity emits two independently triggered entangled photons. The entanglement is mediated by the atom and is characterized both by a Bell inequality violation of $S = 2.5$, as well as full quantum-state tomography, resulting in a fidelity exceeding $F = 90\%$. The combination of cavity-QED and trapped atom techniques makes our protocol inherently deterministic—an essential step for the generation of scalable entanglement between the nodes of a distributed quantum network.

DOI: 10.1103/PhysRevLett.102.030501 PACS numbers: 03.67.Bg, 03.65.Ud, 42.50.Pq, 42.50.Xa

Of all the technologies currently being pursued for quantum information science, individually trapped atoms are among the most proven candidates for quantum information storage [1]. Photons, on the other hand, are the obvious choice for carriers of quantum information over large distances. Together, these naturally lead to an atom-photon interface as an ideal node for distributed quantum computing networks [1–3]. Several recent results have demonstrated entanglement between single atoms trapped in a free-space radiation environment and their spontaneously emitted photons [4,5]; however, high photon loss rates in the emission process severely limit their usefulness for quantum information processing protocols [6]. For *scalable* atom-photon based quantum information processing, it is necessary to increase the entanglement efficiency. The most promising method to accomplish this is to combine the advantages of trapped atom entanglement techniques with cavity quantum electrodynamics where both atomic and photonic qubits are under complete control [3,7–10].

In this Letter, we demonstrate a deterministic entanglement protocol with a single atom trapped in an optical cavity and two subsequently emitted single photons. Compared to previous entanglement experiments with a probabilistic transit of atoms through a cavity [7], our results increase the number of successful atom-photon entanglement events from a single atom by a factor of 10^5. The long trapping times shown here also allow us to ensure that exactly one atom is within the cavity at a given time, which is not possible with atoms randomly loaded into a cavity [7]. Furthermore, the highly efficient photon collection in the cavity output mode allows for photon detection efficiencies that are more than an order of magnitude greater than in free-space atom-photon entanglement experiments [4,5]. This also allows for the coherent mapping of the atomic quantum state onto the state of a second photon. The resulting entanglement is verified by a Bell inequality measurement between the two emitted photons [11], and is in convincing violation of classical physics. While our photon production is currently not deterministic, with ideal cavity, laser cooling, and atom excitation parameters, our protocol would generate entangled photons with unit efficiency.

The main element of our experimental apparatus is a coupled atom-cavity system (Fig. 1). Cold ^{87}Rb atoms are trapped at the intersection of two standing-wave dipole-trap beams—an intracavity beam at 785 nm (trap depth $\approx 30\ \mu$K), which is also used to stabilize the cavity length to the Stark-shifted $D2$ $F = 1 \leftrightarrow F' = 1$ transition, and an orthogonally aligned beam at 1030 nm (≈ 2.3 mK) [8,12].

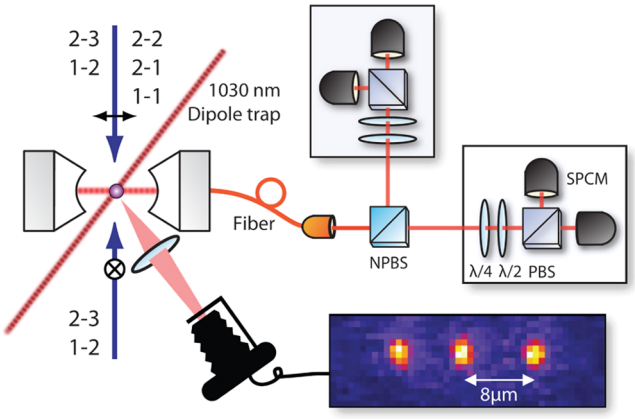

FIG. 1 (color online). Individual ^{87}Rb atoms are trapped within the mode of a high-finesse optical cavity (finesse $\approx 3 \times 10^4$) at the intersection of two standing-wave dipole-trap beams. Lin$\perp$lin-polarized laser beams provide motional cooling, while beams used for the entanglement scheme are polarized along the cavity axis. The 1030 nm dipole-trap beam and all cooling and excitation beams (labeled as i-j, where i and j are the hyperfine quantum numbers F and F' of the $5S_{1/2}$ and $5P_{3/2}$ states, respectively) are perpendicular to the cavity axis. The cavity output is directed to the photonic state detection apparatus. Also perpendicular to the cavity axis, a CCD camera is used to monitor the atoms within the trap. The displayed image shows three atoms coupled to the mode of the cavity and aligned along the 1030 nm beam. SPCM, single photon counting module; NPBS, nonpolarizing beam splitter; PBS, polarizing beam splitter; $\lambda/4$, quarter-wave plate; $\lambda/2$, half-wave plate.

These traps create a measured ac-Stark shift of the atomic $5S_{1/2} \leftrightarrow 5P_{3/2}$ transition frequency of approximately $+95$ MHz.

The atom-cavity system operates in the intermediate coupling regime with $(g, \kappa, \gamma)/2\pi = (5, 6, 3)$ MHz, where g denotes the maximum (spatially dependent) atom-cavity coupling constant of the relevant transitions, κ is the cavity field decay rate, and γ is the atomic polarization decay rate. Once loaded into the cavity mode, the atoms are cooled via lin$\perp$lin-polarized laser beams orthogonal to the cavity axis and near resonant with the $F = 2 \leftrightarrow F' = 3$ and $F = 1 \leftrightarrow F' = 2$ transitions using a Sisyphus-like cooling mechanism [Fig. 2(a)] [12,13]. A laser addressing the $F = 1 \leftrightarrow F' = 1$ transition is also applied for cavity enhanced cooling and to create photons in the cavity mode. Photons emitted from the cavity output are coupled into an optical fiber and directed to the photon detection setup.

For high-fidelity entanglement generation, it is important to ensure that exactly one atom is in the cavity. This is accomplished via two independent techniques. First, we count the number of trapped atoms by directly imaging the cavity region onto a CCD camera (Figs. 1 and 2). A portion of the light scattered by the atoms into free space (perpendicular to the cavity and trapping axes) is collected using an objective lens with a numerical aperture of 0.43 and a measured resolution of 1.3 μm. While this technique alone can determine the number of atoms with over 90% certainty, we can further confirm that exactly one atom is trapped by measuring a perfect photon antibunching signal in the statistics of the emitted photon stream [8]. The combination of these two techniques allows us to discern that a single atom is trapped within the cavity with greater than 99% fidelity.

The experimental procedure follows a similar protocol to that used in [7], but with several substantial differences (Fig. 2). First, the trap-induced Stark shift of the atomic energy levels must be taken into account by detuning the laser and cavity frequencies. Second, the Stark shift has to be stabilized; otherwise fluctuations can lead to unwanted transitions to nearby hyperfine levels of the $P_{3/2}$ manifold. Moreover, a variable detuning of laser and cavity from the atom decreases the photon generation efficiency. Additionally, the unidirectional laser pulses applied in the protocol (discussed below) lead to significant heating of the atom. The resulting atomic motion in the dipole trap shortens the decoherence time [14] as well as expels the atom from the trap within a few milliseconds. We find that by embedding each entanglement sequence with an additional cooling interval [Fig. 2(b)], the atoms remain sufficiently cold to allow for long trapping times and high-fidelity entanglement generation.

After cooling, the entanglement protocol starts by optically pumping the atom into the $|F, m_F\rangle = |2, 0\rangle$ Zeeman sublevel with a measured efficiency greater than 80% [Fig. 2(b)] [15]. Next, entanglement between the atomic Zeeman state and the polarization of the emitted photon is created by driving a vacuum-stimulated Raman adiabatic passage (vSTIRAP) via a π-polarized laser pulse addressing the Stark-shifted $F = 2 \leftrightarrow F' = 1$ transition and the cavity frequency resonant with the $F = 1 \leftrightarrow F' = 1$ transition [Fig. 2(d)] [16]. With a trapped atom coupled to the high-finesse optical cavity, the resulting entanglement is

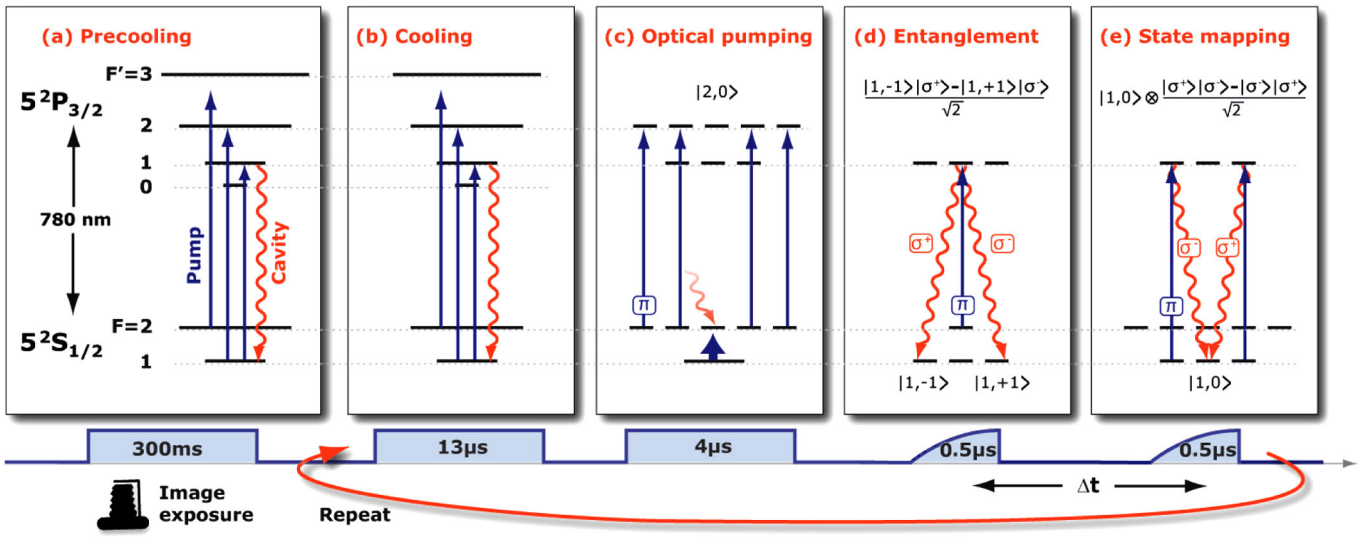

FIG. 2 (color online). The experimental procedure. (a) When atoms are first loaded into the cavity, a 300 ms laser pulse is applied for optical cooling. During this time, a camera images the cavity mode to confirm the presence of a single atom. (b–e) The entanglement generation protocol runs at a repetition rate of 50 kHz. (b) Atomic recooling. (c) A π-polarized laser resonant with the $F = 2 \leftrightarrow F' = 2$ transition together with resonant lasers on the $F = 1 \leftrightarrow F' = 1$ and $F = 1 \leftrightarrow F' = 2$ transitions optically pump the atom to the $|F = 2, m_F = 0\rangle$ Zeeman sublevel. (d) A π-polarized $F = 2 \leftrightarrow F' = 1$ laser transition generates atom-photon entanglement. (e) After a time Δt, a π-polarized $F = 1 \leftrightarrow F' = 1$ laser maps the quantum state of the atom onto a second photon.

inherently deterministic [1,3]:

$$|\Psi_{\mathrm{AP}}\rangle = \frac{1}{\sqrt{2}}(|1,-1\rangle|\sigma^+\rangle - |1,+1\rangle|\sigma^-\rangle). \quad (1)$$

After a user-selected time interval, the atom-photon entanglement is converted into a photon-photon entanglement via a second vSTIRAP step with a π-polarized $F = 1 \leftrightarrow F' = 1$ laser pulse [Fig. 2(e)]. This maps the atomic state onto the polarization of a second emitted photon, resulting in an entangled photon pair:

$$|\Psi_{\mathrm{PP}}^-\rangle = \frac{1}{\sqrt{2}}(|\sigma^+\rangle|\sigma^-\rangle - |\sigma^-\rangle|\sigma^+\rangle). \quad (2)$$

We characterize our entanglement by measuring a Bell inequality violation of the two emitted photons [11]. The form of Bell inequality violated here is based on the expectation value $E(\alpha, \beta)$ of correlation measurements in different bases [17]:

$$E(\alpha,\beta) = p_{\downarrow\downarrow}(\alpha,\beta) + p_{\uparrow\uparrow}(\alpha,\beta) - p_{\uparrow\downarrow}(\alpha,\beta) - p_{\downarrow\uparrow}(\alpha,\beta). \quad (3)$$

Here, $p_{ij}(\alpha, \beta)$ is the probability to contiguously find photon 1 in state $|i\rangle$ and photon 2 in state $|j\rangle$ following polarization rotations by an amount α and β, respectively, and $\{\uparrow, \downarrow\}$ represent the two output ports of the polarizing beam splitter. All local hidden-variable theories must obey the inequality

$$\begin{aligned} S(\alpha,\alpha';\beta,\beta') \equiv\ & |E(\alpha',\beta') - E(\alpha,\beta')| \\ & + |E(\alpha',\beta) + E(\alpha,\beta)| \\ \leq\ & 2. \end{aligned} \quad (4)$$

This inequality can only be violated via quantum physics. In particular, our entangled state $|\Psi_{\mathrm{PP}}^-\rangle$ allows for a Bell signal as large as $2\sqrt{2}$.

In our experiment, the two photons are emitted into the same spatial output mode and are probabilistically directed to two different measurement bases by a 50/50 nonpolarizing beam splitter (Fig. 1), allowing for two simultaneous Bell inequality measurements. To avoid systematic effects during the course of the experiment, the polarization measurement bases are changed before every atom trapping event via motorized rotation stages. Our measurements result in Bell signals of

$$S(0°, 45°; 22.5°, -22.5°) = 2.46 \pm 0.05$$

and $$S(22.5°, -22.5°; 0°, 45°) = 2.53 \pm 0.05,$$

both in clear violation of the classical limit of 2 by more than 9 standard deviations. In this experiment, the photons are temporally separated by 0.8 μs, and the optical path length between the cavity and the photon detectors is 13 m; thus, the first photon is detected before the generation of the second. Nevertheless, the measured correlations can only be explained by quantum entanglement, where the nonclassical information is temporarily stored in the single trapped atom. This is similar to experiments with atomic ensembles where the atomic qubit state must be converted to a photon for measurement [3,18,19].

The entanglement is additionally characterized via quantum-state tomography. For this, we measure the entangled photons in nine different polarization bases [20]. The resulting density matrix for the two photons separated by 0.8 μs is shown in Fig. 3 with an entanglement fidelity of $F = 0.902 \pm 0.009$ with respect to the $|\Psi_{\mathrm{PP}}^-\rangle$ Bell state of the photons [Eq. (2)], clearly above the classical limit of $F = 0.5$. Other measures of entanglement for this state include the concurrence $C = 0.81 \pm 0.03$, entanglement of formation $E_F = 0.73 \pm 0.04$, and logarithmic negativity $E_N = 0.867 \pm 0.014$. They are all significantly above their classical limit of zero and close to their maximum of 1 for a two-qubit state [21]. From the measured density matrix, we can also infer a Bell signal of $S = 2.47 \pm 0.04$, consistent with the results given above.

With atom trapping lifetimes in this experiment of ≈ 4.1 s, the separation between the entangling and mapping pulses is currently limited only by the coherence time of the atomic qubit. By measuring density matrices as a function of time between the two pulses, Δt, we obtain an entanglement lifetime of $\tau_e = 5.7 \pm 0.2$ μs (Fig. 4). This lifetime is limited by phase noise between the two atomic Zeeman states as evidenced by the decreasing off-diagonal coherence terms in the density matrix while the diagonal components remain nearly constant (Figs. 3 and 4). This can also be seen from the decay of the fidelity to 50%, and not 25% as would be the case for a completely mixed state.

Our measured entanglement lifetime is comparable to lifetimes observed in atomic ensemble experiments [3,18,19,22]. In our experiment, the limiting mechanisms are magnetic field instabilities (~20 mG) and a variable differential ac-Stark shift of the atomic superposition states due to motion of the atom, intensity fluctuations of the intracavity trap (~10%), and an uncompensated circular polarization component of the trapping lasers (~2%). With

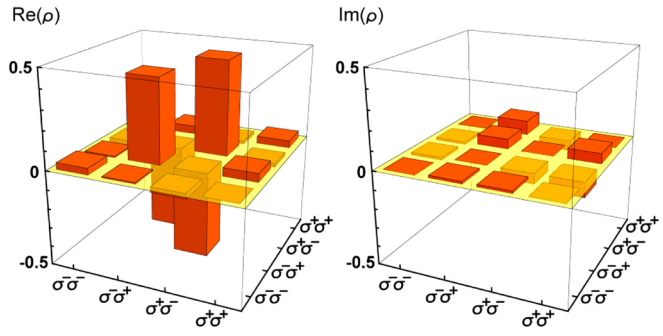

FIG. 3 (color online). Real and imaginary parts of the measured two-photon density matrix. A semitransparent plane at $\rho = 0$ is added to better visualize which elements are positive or negative. This density matrix represents the $|\Psi_{\mathrm{PP}}^-\rangle$ Bell state of the photons with a fidelity of $F = 0.902 \pm 0.009$.

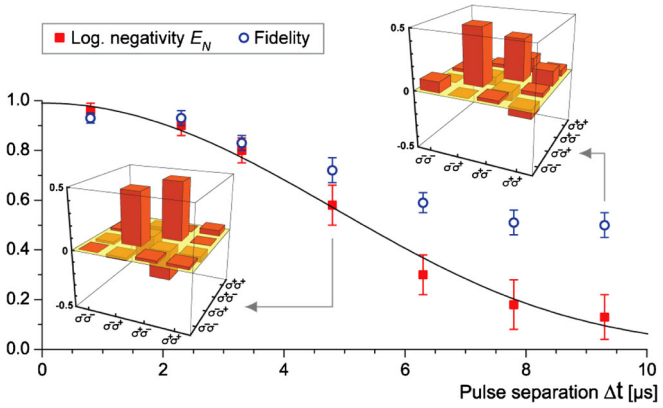

FIG. 4 (color online). Measured fidelity and logarithmic negativity as a function of time between the two vSTIRAP sequences. Note that these data are independent from those shown in Fig. 3. The solid line is a Gaussian fit to the negativity $N(\Delta t)$, displayed as $E_N(\Delta t) = \log_2(2N_0 e^{-(\Delta t/\tau_e)^2} + 1)$, with a resulting entanglement lifetime of $\tau_e = 5.7 \pm 0.2$ μs. The insets show the real parts of the density matrices at differing values of Δt (all imaginary parts have a magnitude smaller than 0.14). The entanglement lifetime is limited mainly by a loss of phase coherence between the $|1, -1\rangle$ and $|1, +1\rangle$ states.

active stabilization of the magnetic field and optimized laser parameters, this lifetime may be increased to over 100 μs [5] or, by converting the atomic qubit to clock states, to even hundreds of ms [14].

The measured fidelity of the entangled state is further limited by imperfect polarization control in the optical path to the detection setup, dark counts of the photon detectors, and multiple scattered photons during the mapping pulse. Indeed, by including photons only from the first 40% of the mapping pulse, the fidelity increases to $F = 0.932 \pm 0.014$, albeit with a reduced coincidence rate. However, with the incorporation of a fast excitation scheme [23] and improved cooling and cavity parameters, many of these effects can be dramatically reduced.

Finally, the most important aspect for scalable atom-photon networking is the overall success probability. Here, with a single atom in the cavity, the probability of detecting a two-photon event is $\approx 2.4 \times 10^{-4}$, as the probabilities for generating single photons into the cavity mode during the entangling and mapping pulses are each $\approx 9\%$, and the detection efficiency for a single photon present inside the cavity is ~ 0.2. This results in ≈ 370 produced entangled two-photon pairs per second, of which ≈ 12 are detected. These values are largely limited by the nonoptimal atom-cavity coupling due to atomic motion, optical pumping inefficiencies, and photon loss mechanisms, including a 50% absorption loss due to a cavity mirror defect. While an atom trapped within an optical cavity can in principle generate photons with unit efficiency [2,3], these results still compare well to free-space single atom entanglement experiments with detection probabilities for two subsequent single photons $< 5 \times 10^{-7}$ [4,5].

Our entanglement scheme may also be extended to many-photon [24] and many-atom entanglement protocols [25–27], as well as schemes for quantum teleportation, quantum repeaters [28], and a loophole-free Bell inequality violation. Finally, with the recent completion of a second, independent, trapped-atom-cavity system in our group [23], the demonstration of highly efficient remote-atom entanglement should be possible in the near future.

The authors thank N. Kiesel and A. Ourjoumtsev for useful discussions. This work was partially supported by the Deutsche Forschungsgemeinschaft (Research Unit 635, Cluster of Excellence MAP) and the European Union (IST project SCALA). D. L. M. acknowledges support from the Alexander von Humboldt Foundation.

*david.moehring@mpq.mpg.de

[1] C. Monroe, Nature (London) **416**, 238 (2002).
[2] J. I. Cirac *et al.*, Phys. Rev. Lett. **78**, 3221 (1997).
[3] H. J. Kimble, Nature (London) **453**, 1023 (2008).
[4] D. N. Matsukevich *et al.*, Phys. Rev. Lett. **100**, 150404 (2008).
[5] W. Rosenfeld *et al.*, Phys. Rev. Lett. **101**, 260403 (2008).
[6] E. T. Campbell and S. C. Benjamin, Phys. Rev. Lett. **101**, 130502 (2008).
[7] T. Wilk *et al.*, Science **317**, 488 (2007).
[8] M. Hijlkema *et al.*, Nature Phys. **3**, 253 (2007).
[9] K. M. Fortier *et al.*, Phys. Rev. Lett. **98**, 233601 (2007).
[10] M. Khudaverdyan *et al.*, New J. Phys. **10**, 073 023 (2008).
[11] J. S. Bell, Physics (Long Island City, N.Y.) **1**, 195 (1964).
[12] S. Nußmann *et al.*, Nature Phys. **1**, 122 (2005).
[13] K. Murr *et al.*, Phys. Rev. A **73**, 063415 (2006).
[14] S. Kuhr *et al.*, Phys. Rev. Lett. **91**, 213002 (2003).
[15] Note that optical pumping to the wrong state will not reduce the measured entanglement fidelity as it cannot result in a two-photon entanglement event [7].
[16] M. Hennrich *et al.*, Phys. Rev. Lett. **85**, 4872 (2000).
[17] J. F. Clauser *et al.*, Phys. Rev. Lett. **23**, 880 (1969).
[18] S. D. Jenkins *et al.*, J. Opt. Soc. Am. B **24**, 316 (2007).
[19] Z.-S. Yuan *et al.*, Nature (London) **454**, 1098 (2008).
[20] J. B. Altepeter, E. R. Jeffrey, and P. G. Kwiat, Adv. At. Mol. Opt. Phys. **52**, 105 (2005).
[21] M. B. Plenio and S. Virmani, Quantum Inf. Comput. **7**, 1 (2007).
[22] J. Simon *et al.*, Nature Phys. **3**, 765 (2007).
[23] J. Bochmann *et al.*, Phys. Rev. Lett. **101**, 223601 (2008).
[24] C. Schön *et al.*, Phys. Rev. Lett. **95**, 110503 (2005).
[25] X.-L. Feng *et al.*, Phys. Rev. Lett. **90**, 217902 (2003).
[26] L.-M. Duan and H. J. Kimble, Phys. Rev. Lett. **90**, 253601 (2003).
[27] D. E. Browne *et al.*, Phys. Rev. Lett. **91**, 067901 (2003).
[28] S. Bose *et al.*, Phys. Rev. Lett. **83**, 5158 (1999).